

Excitonic optical properties in monolayer SnP_2S_6

Peng-Yuan Chen(陈鹏远), Zhen Quan(权真), and Shu-Dong Wang(王舒东)

Citation: Chin. Phys. B, 2024, 33 (**10**): 107105. DOI: 10.1088/1674-1056/ad73b5
Journal homepage: http://cpb.iphy.ac.cn; http://iopscience.iop.org/cpb

What follows is a list of articles you may be interested in

Strain tunable excitonic optical properties in monolayer Ga_2O_3

Hao-Lei Cui(崔浩磊), Zhen Quan(权真), and Shu-Dong Wang(王舒东)
Chin. Phys. B, 2024, 33 (**10**): 107104. DOI: 10.1088/1674-1056/ad74e7

Exciton-polaritons in a 2D hybrid organic-inorganic perovskite microcavity with the presence of optical Stark effect

Kenneth Coker, Chuyuan Zheng(郑楚媛), Joseph Roger Arhin, Kwame Opuni-Boachie Obour Agyekum, and Weili Zhang(张伟利)
Chin. Phys. B, 2024, 33 (**3**): 037102. DOI: 10.1088/1674-1056/ad1484

Dynamic recombination of triplet excitons in polymer heterojunctions

Ya-Dong Wang(王亚东), Jian-Jun Liu(刘建军), Xi-Ru Wang(王溪如), Yan-Xia Liu(刘艳霞), and Yan Meng(孟艳)
Chin. Phys. B, 2020, 29 (**11**): 117101. DOI: 10.1088/1674-1056/ab9c13

Exciton optical absorption in asymmetric ZnO/ZnMgO double quantum wells with mixed phases

Zhi-Qiang Han(韩智强), Li-Ying Song(宋丽颖), Yu-Hai Zan(昝宇海), Shi-Liang Ban(班士良)
Chin. Phys. B, 2020, 29 (**7**): 077104. DOI: 10.1088/1674-1056/ab8d9d

Effect of disorder on exciton dissociation in conjugated polymers

Yuwen Feng(冯誉雯), Hui Zhao(赵晖), Yuguang Chen(陈宇光), Yonghong Yan(鄢永红)
Chin. Phys. B, 2017, 26 (**10**): 107103. DOI: 10.1088/1674-1056/26/10/107103

Excitonic optical properties in monolayer SnP_2S_6

Peng-Yuan Chen(陈鹏远), Zhen Quan(权真), and Shu-Dong Wang(王舒东)†

School of Physical Science and Technology, Inner Mongolia University, Hohhot 010021, *China*

(Received 18 July 2024; revised manuscript received 20 August 2024; accepted manuscript online 27 August 2024)

Quantum confinement effect and reduced dielectric screening in two-dimensional (2D) dramatically enhance the electron–hole interactions. In this work, we use many-body perturbation theory and Bethe–Salpeter equation (BSE) to investigate the electronic and excitonic optical properties of monolayer SnP_2S_6. Our findings reveal that the excitonic effect dominates the optical absorption spectra in the visible light range, and the lowest-energy exciton X_0 in monolayer SnP_2S_6 is optically bright with the binding energy of 0.87 eV and the radiative lifetime of $\sim 10^{-11}$ s, which is highly advantageous to the photo-luminescence. Most importantly, the absence of optically forbidden states below the bright states X_0 would give rise to a high quantum efficiency of 2D SnP_2S_6. We also find that applied biaxial strain can further shorten the radiative lifetime of the bright states. These results imply that 2D SnP_2S_6 is a promising candidate for the optoelectronic devices.

Keywords: excitons, radiative lifetime, SnP_2S_6

PACS: 71.35.–y, 71.35.Cc, 31.15.ag, 73.43.Cd **DOI:** 10.1088/1674-1056/ad73b5

1. Introduction

Two-dimensional (2D) materials have attracted lots of attention since the successful exfoliation of graphene.[1] Among all the 2D materials, semiconductors exhibit strong light–mater coupling due to the quantum confinement and the reduced dielectric screening effects. For instance, during low-energy optical excitation processes, the strongly bounded electron–hole pairs, e.g., excitons, dominate the absorption and photo-luminescence spectra, even at room temperature due to the large exciton binding energy.[2–4] Excitons are also responsible for the valley properties of transition metal dichalcogenides (TMDs),[4–6] and the various novel quantum states at low temperatures.[7,8] Meanwhile, the stable TMDs under ambient conditions provide an opportunity to optically manipulate spin-valley properties.

Recently, a new metal chalcogenophosphates layered material MP_2X_6 (M = metal, X = S, Se) attract our attention with intermediate band gaps between TMDs and boron nitride (1.6 eV–4.0 eV).[9–11] Among them, SnP_2S_6 as a promising nonlinear optical (NLO) material[12] has gained more attention. Zhang *et al.*[13] reported the strong second-harmonic (SH) response of SnP_2S_6, which is 1–2 orders of magnitude higher than that of other discovered 2D materials. They also found obvious self-trapped excitons emission in 2D SnP_2S_6 crystals caused by structural distortion and strong electron–phonon interaction.[14] He *et al.*[15] revealed as well the large SH susceptibility of SnP_2S_6 bulk single crystal. The pressure dependence of the structural and electronic properties, including piezoelectric, ferroelectric, thermoelectric, and superconductivity of SnP_2S_6 layered semiconductor has been investigated.[16–18] Recent studies have shown that SnP_2S_6 posses high carrier mobility, higher dielectric constant than that of hexagonal boron nitride and is a potential photocatalyst for solar water splitting.[19–22] The intermediate band gap, good photoresponse properties, and strong NLO effect make 2D SnP_2S_6 a good candidate for future optoelectronic devices.

For light–mater interaction from the theoretical perspective, especially for the absorption and emission process, accurate understanding of the electronic structures including quasi-particle (QP) self-energy corrections is required. Here, based on many-body perturbation theory[23] we firstly discuss the QP energies of monolayer SnP_2S_6, and then the optical spectra including excitonic effect are calculated from the Bethe–Salpeter equation (BSE).[24,25] Following that, we demonstrate the exciton radiative lifetime and brightness of the excitons to the quantum yield. Finally, applying mechanical strain to SnP_2S_6, we present the changes of the excitonic states under various strains.

2. Computational and theoretical methods

The ground state calculations are performed using Quantum-ESPRESSO package.[26,27] The exchange–correlation potentials are treated by the generalized gradient approximation (GGA) with the Perdew–Burke–Ernzerhof (PBE) functional.[28] The wavefunctions are expanded on a plane-wave basis set with a kinetic energy cutoff of 80 Ry (1 Ry = 13.6056923(12) eV), and a Monkhorst–Pack mesh of 18×18×1 k-points is adopted. The optimized norm-conserving Vanderbilt pseudopotentials from PseudoDojo[29,30] are taken into account for the valence electrons. The vacuum thickness is set to 20 Å to mimic the isolated system.

†Corresponding author. E-mail: sdwang@imu.edu.cn

© 2024 Chinese Physical Society and IOP Publishing Ltd

Based on the ground states results, the quasi-particle energies E^{QP} are computed within the one-shot GW approximation (G_0W_0) by

$$E^{\mathrm{QP}} = E^{\mathrm{KS}} + \langle \Psi | \Sigma(E^{\mathrm{QP}}) - V_{\mathrm{xc}} | \Psi \rangle, \tag{1}$$

where V_{xc} is the exchange–correlation potential of density functional theory and self-energy $\Sigma = \mathrm{i}GW$ is the product of the noninteracting one-electron Green's function G and the screened Coulomb potential W. The plasmon-pole approximation[31] is used to treat the screening W. A 60-Ry energy cutoff is taken for exchange part and 14-Ry cutoff for correlation part, and 370 empty bands plus an extrapolar correction scheme[32] is used to ensure the converge.

The electron–hole interaction is obtained by solving the Bethe–Salpeter equation[24,25]

$$(E_{ck} - E_{vk})A^{\mathrm{S}}_{vck} + \sum_{k'v'c'} \langle vck | K^{\mathrm{d}} + 2K^{\mathrm{x}} | v'c'k' \rangle A^{\mathrm{S}}_{v'c'k'} = \Omega^{\mathrm{S}} A^{\mathrm{S}}_{vck}, \tag{2}$$

where E_{ck} and E_{vk} are the quasi-particle energies of the conduction and valence states, and Ω^{S} and A^{S}_{vck} represent the eigenvalues and wavefunctions of excited states, respectively. K^{d} and K^{x} is the direct and repulsive exchange term of the electron–hole interaction, respectively.[24,25] If omit exchange term K^{x}, then we can obtain the spin-triplet excitations.[25] The optical absorption spectra are computed including 5 valence and 5 conduction bands around the band edges. A k-point grid of $42\times42\times1$ is used for the GW calculation and a $48\times48\times1$ k-point grid for BSE calculation. All the excited properties calculations are done with Yambo code.[33,34]

The radiative lifetime of exciton is depicted by the Fermi golden rule.[35,36] At 0 K, the radiative lifetime is

$$\tau_{\mathrm{S}}(0) = \gamma_{\mathrm{S}}(0)^{-1} = \frac{\hbar^2 cA}{8\pi e^2 E_{\mathrm{S}}(0)\mu_{\mathrm{S}}^2}, \tag{3}$$

where c is the speed of light, A is the area of the unit cell, $E_{\mathrm{S}}(0)$ is the excitation energy, and μ_{S} is the transition dipole moment of the exciton. For non-zero temperature, the lifetime is given by

$$\langle \tau_{\mathrm{S}} \rangle(T) = \gamma_{\mathrm{S}}(0)^{-1} \times \frac{3}{4}\left(\frac{2M_{\mathrm{S}}c^2 k_{\mathrm{B}}T}{E_{\mathrm{S}}(0)^2}\right), \tag{4}$$

where k_{B} is the Boltzmann constant and M_{S} is the effective mass of the exciton deduced from the quasi-particle energies.

3. Results and discussion

Figure 1(a) is the geometry of the relaxed monolayer SnP_2S_6. The lattice parameter we calculated is $a = b = 5.967$ Å, which is slightly smaller than the experimental value of the bulk SnP_2S_6 (5.999 Å).[15] The band structures are shown in Fig. 1(b). As can be seen, the monolayer SnP_2S_6 is a direct band gap semiconductors, with both the valence band maximum (VBM) and conduction band minimum (CBM) locating at the K point of the hexagonal Brillouin zone. The calculated PBE band gap is 1.31 eV, while the quasi-particle band gap with G_0W_0 approximation is 2.84 eV, meaning the GW self-energy corrections play a dominant role in the electronic structures. We also notice that there exits band stretching for GW results comparison to the PBE one, resulting in a more significant band dispersion and thus the smaller electron and hole effective mass. Figure 1(c) illustrates the charge densities of VBM-1 to CBM+1. VBM-1 is composed of p orbital of S atoms, and also the σ bond between the two P atoms. VBM is dominated by the p orbital of S atoms. CBM mixes the p orbital of S atoms and s orbital of Sn atom. CBM+1 is more complicated, arising from the σ^* antibonding orbital of P atoms and the s–p hybrid orbitals of the S atoms.

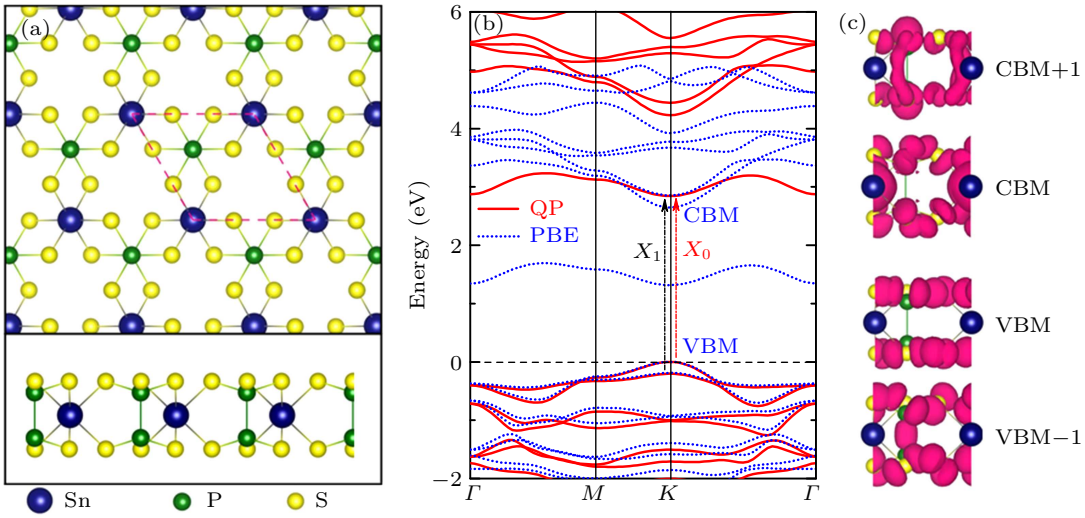


Fig. 1. (a) Top and side views of monolayer SnP_2S_6. The primitive cell is shown by the dashed lines. (b) Quasiparticle (red solid line) and PBE (blue short-dashed line) band structures. The vertical arrow lines illustrate the interband transitions of exciton X_0 and X_1. The Fermi energy is set zero. (c) Charge density of valence (VBM, VBM-1) and conduction (CBM, CBM+1) bands.

Figure 2 shows the absorption spectra of SnP_2S_6 with the incident light in the direction of (1,1,0), e.g., the electric field vector of light within the plane of 2D SnP_2S_6. The shaded area is the absorption with the random phase approximation (RPA) neglecting the electron–hole interaction, where the continuous absorption threshold is at the 2.84 eV, which is also the quasi-particle gap of SnP_2S_6. When the electron–hole interaction has been taken into accounted through solving the BSE equation on top of G_0W_0 quasi-particle energies, the absorption spectra experiences a significant red shift compared to the *GW*+RPA results, accompanying with the remarkable enhancement of the absorption intensity, as illustrated by the orange line in Fig. 2. All the absorption components below the continuous absorption threshold originate from the electron–hole interaction, e.g., the excitonic effect. The lowest-energy exciton X_0, located at 1.97 eV in Fig. 2, is a bright one contributed by the transition between the VBM and CBM at the K point. The binding energy of X_0 is 0.87 eV, meaning the X_0 is very stable at room temperature. The stable, lowest-energy bright exciton is highly advantageous to the photo luminescence, since the photoexcited electrons can decay radiatively without passing the optically dark states below the optical gap. The X_1 at 2.08 eV, coming from the transition between the VBM-1 and CBM, has much larger oscillator strength than X_0, and there is no other photoexcited energy levels observed between X_0 and X_1. The absence of optically forbidden states, i.e., dark states, below the bright states X_0 and X_1 would give rise to a high quantum efficiency of 2D SnP_2S_6. Actually, group theory predicts that the brightness of the states X_0 and X_1 originating from the allowed dipolar transitions with the light vector along the plane of the layer (xy plane). The bands of 2D SnP_2S_6 at the K point belongs to C_3. For VB at K, the irreducible representations of S p_x and p_y is E according to the character table. For CB at K, p_x and p_y orbitals of S are E, and p_z is A, and s orbital of Sn is A. For VB $\rightarrow$ CB, $E \otimes E = 2A + E$, $E \otimes A = E$, and thus for in-plane light vector E, the product of the irreducible representations of the polarization direction and the initial and final states contain the totally symmetric irreducible representation A, which is dipole-allowed in principle. Similar considerations hold also for the VB-1$\rightarrow$ CB transition. The calculated radiative lifetime of X_0 is 1.63×10^{-11} s at 0 K (1.01×10^{-7} s at 300 K), while it is short as 2.11×10^{-12} s (1.48×10^{-8} s at 300 K) for X_1 due to the larger oscillator strength.

To further analyse the exciton characteristic of the low energy bright excitons, we explore the exciton spatial distribution written as $|\Psi^S(r_e, r_h)\rangle = \sum_{cvk} A^S_{cvk} \psi_{ck}(r_e)\psi^*_{vk}(r_h)$, where r_e and r_h are the coordinates in real-space for exciton S, respectively. The ψ_{cv} and ψ_{vk} is the quasi-electron and quasi-hole wave function, and A^S_{cvk} is the exciton composition in terms of electron–hole pairs. Figure 3 illustrates the real-space exciton wave functions of X_0 and X_1. The strong overlap of the electron and hole wave functions of X_1 leads to a more localized real-space exciton than in X_0, as shown in Fig. 5. According to the orbital characteristics involved in transition, we fixed the hole around S atom here.

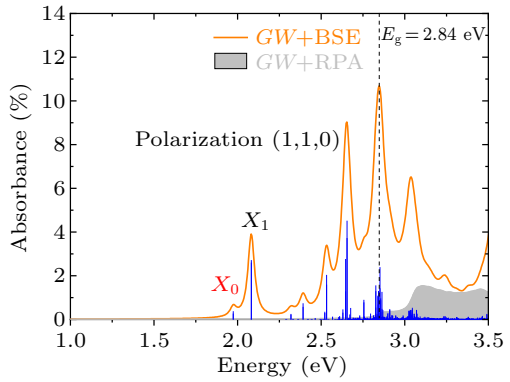


Fig. 2. Absorption spectra with the incident light in direction of (1, 1, 0) with (*GW*+BSE) and without (*GW*+RPA) excitonic effects. The oscillator strength is denoted by the vertical lines.

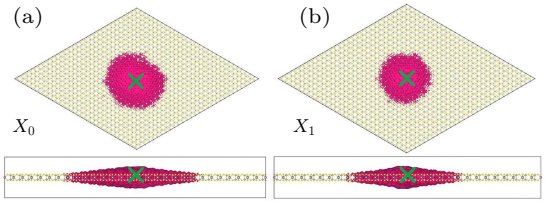


Fig. 3. Exciton wave functions of (a) X_0 and (b) X_1. The upper (lower) panels are the top (side) views. The hole position is fixed around S atom denoted by the cross. The isosurface values are the same for both X_0 and X_1.

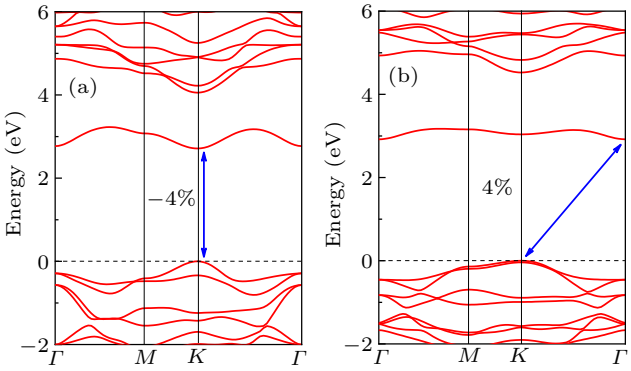


Fig. 4. Quasi-particle band structures with biaxial strain of (a) −4% and (b) 4%.

Strain effects have a substantial influence on the electronic band structure, transport and optical properties, especially for atomic-thick 2D structures.[37,38] Figure 4 shows the quasi-particle band structures of monolayer SnP_2S_6 with applied biaxial compressive and tensile strain. The quasi-particle band gap with compressive strain of −4% is 2.71 eV, exhibiting a band gap reduction of 0.13 eV compared to the strain-free SnP_2S_6. Meanwhile the band splitting between VB and VB-1 at the K point is larger than in that of strain-free SnP_2S_6.

On the contrary, the 4% tensile strain bring about a transition from indirect band gap to direct band gap semiconductor for SnP_2S_6. As shown in Fig. 4(b), the direct (at the K point) and indirect band gap (between K and Γ) are 2.94 eV and 3.04 eV, respectively. Another striking feature of the quasi-particle band structure is that the VB and VB-1 at the K point almost degenerate under the tensile strain, accompanying with less dispersive CB+1, VB and VB-1 energy bands.

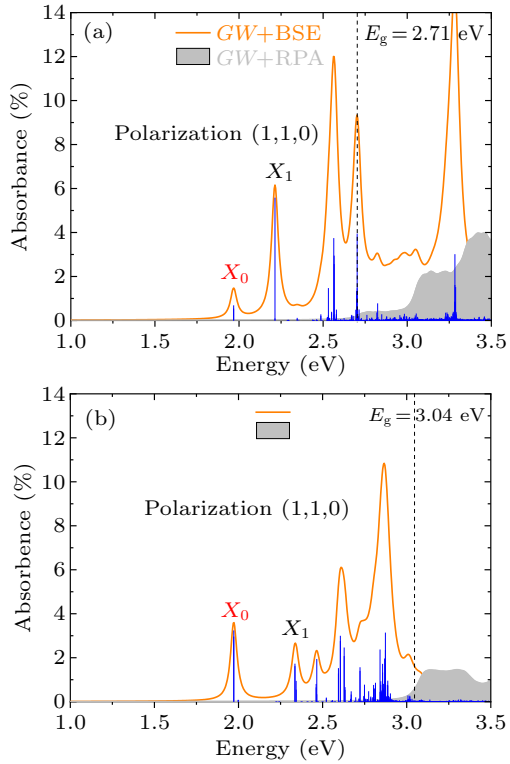


Fig. 5. Absorption spectra under (a) −4% compressive strain and (b) 4% tensile strain, with the incident light in direction of (1, 1, 0).

In Fig. 5 we present the absorption spectra under strains. In comparison to the spectrum of strain-free case, the excitation energy difference, for −4% compressive strain in Fig. 5(a), between X_0 (at 1.96 eV) and X_1 (at 2.21 eV) is large due to the enhanced energy splitting between VB and VB-1. The calculated radiative lifetime of X_0 is 5.69×10^{-12} s at 0 K (2.46×10^{-8} s at 300 K), while it is 6.03×10^{-13} s at 0 K (1.82×10^{-9} s at 300 K) for X_1, one order of magnitude shorter than that in pristine SnP_2S_6. For 4% tensile strain, as shown in Fig. 5(b), the oscillator strength of X_0 (at 1.97 eV) is greater than X_1 (at 2.34 eV), owing to the order of VB and VB-1 is inverted here compared to the strain-free structure. The increase in band gap will lead to an enhancement in exciton binding energy, resulting in a red-shift in the absorption spectrum. In this way, the increased band gap and the red-shift spectra will cancel each other out, making X_0 appear unchanged here. The X_1 is contributed from the transitions between VB and CB along the path of the K to M point. At 0 K, the radiative lifetime of X_0 is 2.36×10^{-12} s (1.78×10^{-8} s at 300 K), which is more than two times shorter than that of in −4% compressive case, and likewise one order of magnitude shorter than that in pristine SnP_2S_6. For X_1 in Fig. 5(b), the radiative lifetime is 3.72×10^{-12} s at 0 K (2.0×10^{-8} s at 300 K), slightly longer than X_0.

4. Conclusion

In summary, we have theoretically investigated electronic and excitonic optical properties of monolayer SnP_2S_6. We reveal that the excitonic effect dominates the optical absorption spectra, and the lowest-energy exciton X_0 in monolayer SnP_2S_6 is optically bright with the binding energy of 0.87 eV, meaning it is very stable at room temperature. The stable, lowest-energy bright exciton is highly advantageous to the photo-luminescence. The higher excitation exciton at 2.08 eV has much larger oscillator strength than X_0. Most importantly, the absence of optically forbidden states below the bright states X_0 and X_1 would give rise to a high quantum efficiency of 2D SnP_2S_6. We also find that applied biaxial strain can further shorten the radiative lifetime of the bright states X_0 and X_1. These results imply that 2D SnP_2S_6 is a promising candidate for the optoelectronic devices.

Acknowledgement

Project support by the National Natural Science Foundation of China (Grant No. 12064032).

References

[1] Novoselov K S, Geim A K, Morozov S V, Jiang D, Zhang Y, Dubonos S V, Grigorieva I V and Firsov A A 2004 *Nature* **306** 666
[2] Chernikov A, Berkelbach T C, Hill H M, Rigosi A, Li Y, Aslan B, Reichman D R, Hybertsen M S and Heinz T F 2018 *Phys. Rev. Lett.* **113** 076802
[3] Qiu D Y, da Jornada F H and Louie S G 2016 *Phys. Rev. B* **93** 235435
[4] Wang G, Chernikov A, Glazov M M and Heinz T F 2018 *Rev. Mod. Phys.* **90** 021001
[5] Manzeli S, Ovchinnikov D, Pasquier D, Yazyev O V and Kis A 2017 *Nat. Rev. Mater.* **2** 17033
[6] Schaibley J R, *et al.* 2016 *Nat. Rev. Mater.* **1** 16055
[7] Wang Z, *et al.* 2019 *Nature* **574** 76
[8] Andrei E Y, *et al.* 2021 *Nat. Rev. Mater.* **6** 201
[9] Zhang X, Zhao Z, Wu D, Jing Y and Zhou Z 2016 *Adv. Sci.* **3** 1600062
[10] Chittari B L, Park Y, Lee D, Han M, Macdonald A H, Hwang E and Jung J 2016 *Phys. Rev. B* **94** 184428
[11] Lee J U, Lee S, Ryoo J H, Kang S, Kim T Y, Kim P, Park C H, Park J G and Cheong H 2016 *Nano Lett.* **16** 7433
[12] Wang Z, Willett R D, Laitinen R A and Cleary D A 1995 *Chem. Mater.* **7** 856
[13] Zhang Y, Wang F, Feng X, Sun Z, Su J, Zhao M, Wang S, Hu X and Zhai T 2022 *Nano Res.* **15** 2391
[14] Zhang Y, Wang F, Feng X, Zheng Z, Liu K, Xia F, Liang W, Hu X, Ma Y, Li H, Xing G and Zhai T 2022 *Adv. Funct. Mater.* **32** 2205757
[15] He J, Lee S H, Naccarato F, Brunin G, Zu R, Wang Y, Miao L, Wang H, Alem N, Hautier G, Rignanese G M, Mao Z and Gopalan V 2022 *ACS Photon.* **9** 1724
[16] RushchanskiiK Z, Vysochanskii Y M, Cajipe V B and Bourdon X 2006 *Phy. Rev. B* **73** 115115
[17] Shchennikov V V, Morozova N V, Tyagur I, Tyagur Y and Ovsyannikov S V 2011 *Appl. Phys. Lett.* **99** 212104

[18] Karaca E and Errandonea D 2024 *Results in Physics* **57** 107330
[19] Lin M, Liu P, Wu M, Cheng Y, Liu H, Cho K, Wang W H and Lu F 2019 *Appl. Surf. Sci.* **493** 1334
[20] Jing Y, Zhou Z, Zhang J, Huang C, Li Y and Wang F 2019 *Phys. Chem. Chem. Phys.* **21** 21064
[21] Hattori Y, Taniguchi T, Watanabe K and Nagashio K 2015 *ACS Nano* **9** 916
[22] Hu J, Zheng A, Pan E, Chen J, Bian R, Li J, Liu Q, Cao G, Meng P, Jian X, Molnar A, Vysochanskii Y and Liu F 2022 *J. Mater. Chem. C* **10** 13753
[23] Hedin L 1965 *Phys. Rev.* **139** A796
[24] Albrecht S, Reining L, Del Sole R and Onida G 1998 *Phys. Rev. Lett.* **80** 4510
[25] Rohlfing M and Louie S G 2000 *Phys. Rev. B* **62** 4927
[26] Giannozzi P, Andreussi O, Brumme T, Bunau O, Buongiorno Nardelli M, Calandra M, Car R, Cavazzoni C, Ceresoli D, Cococcioni M, *et al.* 2017 *J. Phys.: Condens. Matter* **29** 465901
[27] Giannozzi P, Baroni S, Bonini N, Calandra M, Car R, Cavazzoni C, Ceresoli D, Chiarotti G L, Cococcioni M, Dabo I, *et al.* 2009 *J. Phys.: Condens. Matter* **21** 395502
[28] Perdew J P, Burke K and Ernzerhof M 1996 *Phys. Rev. Lett.* **77** 3865
[29] Hamann D R 2013 *Phys. Rev. B* **88** 85117
[30] van Setten M J, Giantomassi M, Bousquet E, Verstraete M J, Hamann D R, Gonze X and Rignanese G M 2018 *Comput. Phys. Commun.* **226** 39
[31] Godby R W and Needs R J 1989 *Phys. Rev. Lett.* **62** 1169
[32] Bruneval F and Gonze X 2008 *Phys. Rev. B* **78** 085125
[33] Marini A, Hogan C, Grüning M and Varsano D 2009 *Comput. Phys. Commun.* **180** 1392
[34] Sangalli D, Ferretti A, Miranda H, Attaccalite C, Marri I, Cannuccia E, Melo P, Marsili M, Paleari F, Marrazzo A, *et al.* 2019 *J. Phys.: Condens. Matter* **31** 325902
[35] Palummo M, Bernardi M and Grossman J C 2015 *Nano Lett.* **15** 2794
[36] Chen H Y, Jhalani V A, Palummo M and Bernardi M 2019 *Phys. Rev. B* **100** 075135
[37] Yun W S, Han S W, Hong S C, Kim I G and Lee J D 2012 *Phys. Rev. B* **85** 033305
[38] Song W and Yang L 2017 *Phys. Rev. B* **96** 235441